Magnitude of the CH/π Interaction in the Gas Phase: Experimental and Theoretical Determination of the Accurate Interaction Energy in Benzene-methane

Kenta Shibasaki,[†] Asuka Fujii,*[,†] Naohiko Mikami,[†] and Seiji Tsuzuki*[,‡]

Department of Chemistry, Graduate School of Science, Tohoku University, Sendai 980-8578, Japan, and National Institute of Advanced Industrial Science and Technology (AIST), Tsukuba, Ibaraki 305-8568, Japan

Received: January 27, 2006

The accurate CH/π interaction energy of the benzene−methane model system was experimentally and theoretically determined. In the experiment, mass analyzed threshold ionization spectroscopy was applied to the benzene−methane cluster in the gas phase, prepared in a supersonic molecular beam. The binding energy in the neutral ground state of the cluster, which is regarded as the CH/π interaction energy for this model system, was evaluated from the dissociation threshold measurements of the cluster cation. The experimentally determined binding energy (D_0) was 1.03−1.13 kcal/mol. The interaction energy of the model system was calculated by ab initio molecular orbital methods. The estimated CCSD(T) interaction energy at the basis set limit (D_e) was −1.43 kcal/mol. The calculated binding energy (D_0) after the vibrational zero-point energy correction (1.13 kcal/mol) agrees well with the experimental value. The effects of basis set and electron correlation correction procedure on the calculated CH/π interaction energy were evaluated. Accuracy of the calculated interaction energies by DFT methods using BLYP, B3LYP, PW91 and PBE functionals was also discussed.

I. Introduction

An attractive interaction between a C−H bond and a π electron system has been subject to a number of studies in various fields of chemistry.[1−59] Nishio and co-workers first pointed out the existence of such a weak interaction on the basis of the preferential contact between bulky alkyl and phenyl groups, and they called it the "CH/π interaction".[6−16] The CH/π interaction is supposed to be a crucial driving force in the molecular recognition and in the crystal packing of organic compounds.[17−39] Because of the universality of both alkyl and phenyl groups in biorelated molecules, this interaction is believed to play important roles in many biological systems.[1,2,40−42] In addition, the effect of the CH/π interaction in liquid crystals has also been discussed with respect to their alignment functions.[43]

In contrast to the broad interests in the CH/π interaction, its physical origin has not yet been fully understood. The CH/π interaction locates on the gray area between the weakest class of hydrogen bonds and the van der Waals force. The energy decomposition of the CH/π interaction and the resultant contribution of the electrostatic and charge transfer terms have been in controversy, as rather early theoretical studies had predicted the importance of these two terms.[1,6,44,45] Recent high-level ab initio calculations, however, showed that the dispersion is the major source of attraction in the CH/π interaction.[46−49]

For understanding of the nature of the CH/π interaction, determination of its accurate interaction energy seems to be very essential. The magnitude of the interaction energy is the most important physical quantity to characterize the intermolecular interaction. In addition, the accurate interaction energy is strongly desired to construct a force field including the CH/π interaction. Recently, theoretical calculations of the CH/π interaction energy were reported.[46−58] The magnitude of the calculated interaction energy highly depends on the calculation level. Therefore, the comparison with an experimental interaction energy is an effective test for the reliability of theoretical calculations.

Hirota and co-workers measured the enthalpies of the C_6D_6−$CHCl_3$ and C_6D_6−CH_2Cl_2 complex formation in the CCl_4 solution,[59] whereas the measurement of the CH/π interaction energy in the gas phase has not yet been reported. A variety of intermolecular interactions competes in a bulk phase, and such congestion prevents us from the extraction only of the accurate CH/π interaction energy from the total interaction energy of the system. On the other hand, the intermolecular interaction is very simplified in an isolated binary cluster in the gas phase. Therefore, binary clusters are ideal model systems for the characterization of weak intermolecular interactions such as CH/π interaction. The benzene−methane cluster is especially important for the study of the CH/π interaction because this cluster is of the most fundamental combination of the aromatics and hydrocarbons. The binding energy of this cluster can be regarded as a typical CH/π interaction energy.

The benzene−methane cluster in the gas phase was first studied by Schauer and Bernstein with electronic spectroscopy.[60] The S_1−S_0 origin band of the benzene moiety was absent in this cluster, and they concluded the cluster structure where the methane molecule locates on the C_6 axis of the benzene moiety to hold the C_3 or effectively higher symmetry. Tsuzuki et al. performed high-level ab initio calculations of the benzene−methane cluster as the most typical system for the CH/π interaction.[47] They confirmed that the on-top type isomer indicated by the electronic spectroscopy is the most stable structure and evaluated the interaction energy in the cluster at various calculation levels. They reported that the binding energy

* Corresponding authors. E-mail: A.F., asuka@qclhp.chem.tohoku.ac.jp; S.T., s.tsuzuki@aist.go.jp.
† Tohoku University.
‡ AIST.

10.1021/jp0605909 CCC: $33.50
Published on Web 03/16/2006

from the bottom of the potential (D_e) is 1.45 kcal/mol from the estimated CCSD(T) level interaction energy at the basis set limit [$E_{CCSD(T)(limit)}$]. Later on, Takahashi et al. evaluated $D_e = 1.01$ kcal/mol for the same on-top structure by the MP2/6-311++G-(d, p) level calculations.[50]

In the present paper, we applied the mass analyzed threshold ionization (MATI) technique to the benzene−methane cluster and demonstrated the first experimental determination of the accurate CH/π interaction energy. The MATI technique has been widely applied for various types of clusters to evaluate their binding energies.[61−64] In MATI spectroscopy, the dissociation threshold of a cluster in the cationic state is determined by the vibrational energy dependence of the ion appearance channels. The binding energy in the neutral ground state measured from the zero vibrational level (D_0) is evaluated with the dissociation threshold and ionization potential of the cluster. In addition to the binding energy of the benzene-h_6−methane cluster, that of the benzene-d_6−methane cluster was also determined. In collaboration with the experimental measurements, the previously calculated interaction energy of the benzene−methane cluster was revisited in the present work.[47] The geometry of the cluster was fully optimized. The MP2 interaction energy at the basis set limit [$E_{MP2(limit)}$] was estimated using both Helgaker's and Feller's methods for evaluating the effects of the extrapolation procedure.[65,66] Both the cc-pVXZ and aug-cc-pVXZ (X = D, T and Q) basis sets were used for the estimation of the $E_{MP2(limit)}$ to confirm the effects of diffuse functions. The improved CCSD-(T) correction term and zero-point vibrational energies were used for the estimation of the binding energy. The effects of basis set and electron correlation correction procedure on the calculated CH/π interaction energy were discussed to confirm which level of ab initio calculations is necessary for quantitative evaluation of the CH/π interaction energy. We also discussed the accuracy of the calculated CH/π interaction energy by DFT methods.

II. Experiments

MATI spectra of bare benzene and the benzene−methane cluster in a molecular beam were observed. The basic principle of MATI spectroscopy was described in refs 61−64. A supersonic jet expansion of the gaseous mixture of benzene, methane, and buffer Ne was collimated by a skimmer located at 20 mm downstream from the pulsed nozzle orifice. The resultant molecular beam was introduced into the ion extraction stage of a time-of-flight mass spectrometer of the Wiley−McLaren type. Bare benzene or the benzene−methane cluster in the molecular beam was pumped to the long-lived high Rydberg states just below an ionization threshold by the two-color two-photon (1+1′) process via the S_1 6^1 level of the benzene moiety. The prompt ions (ions produced by the direct ionization or by the fast autoionization) were spatially separated from the neutral long-lived Rydberg molecules (clusters) by the weak static electric field of 2.0−8.0 V/cm. After 7 μs from the laser excitation, a pulsed acceleration field of 600 V/cm was applied to the interaction region. The long-lived Rydberg molecule (cluster) was field ionized with this acceleration field. The resultant ion was extracted into the time-of-flight tube with the prompt ions. All the ions were mass-analyzed and were detected by the electron multichannel plate. Because of the spatial separation by the static field, the time-of-flight of the ion due to the pulsed-field ionization of the high Rydberg state (so-called MATI ion) is different from that of the prompt ion of the same mass, and these two ion signals can be temporally distinguished. Only the MATI ion signal was selectively accumulated by the gated boxcar integrator and was processed by the personal computer.

A MATI spectrum is measured by fixing the first excitation laser wavenumber (ν_1) while scanning the second excitation laser wavenumber (ν_2). The MATI signal is produced when the ν_2 laser pumps the molecule (cluster) from the S_1 state to the high Rydberg state just below an ionization threshold (i.e., vibrational level of the cationic ground state). Thus, a MATI spectrum represents the ion−S_1 transition. In the case of clusters, the ion core of the high Rydberg state dissociates when the vibrational energy of the ion core exceeds the dissociation threshold. The Rydberg electron locates so far away from the ion core that the dissociation threshold of the ion core is virtually the same as that of the corresponding cluster cation. Moreover, the Rydberg electron behaves as a spectator for the dissociation process of the ion core, and the Rydberg state of the monomer is produced as a result of the dissociation. The appearance channel of the MATI ion of the cluster switches from the parent cluster ion to the daughter fragment ion (monomer ion) when the vibrational energy of the ion core exceeds the dissociation threshold of the cluster ion. The binding energy of the cluster in the neutral ground state is evaluated from the dissociation threshold of the cation and the ionization potential.

Aromatic samples (benzene-h_6 and benzene-d_6) were purchased from Tokyo Kasei Co. and Aldrich Co., respectively, and were used without further purification. The vapor the aromatic sample was seeded in a neon/methane gaseous mixture with the stagnation pressure of 2−4 atm. The methane concentration was adjusted to be 15−20%, and the vapor pressure of the aromatic sample was controlled by the sample reservoir temperature for the optimization of the cluster signal intensity.

III. Theoretical Calculations

Intermolecular interaction energy of the benzene−methane cluster was calculated by ab initio molecular orbital methods using the Gaussian 03 program.[67] The basis sets implemented in the program were used. Electron correlation was accounted by the second-order Møller−Plesset perturbation (MP2) method,[68,69] by coupled cluster calculations with single and double substitutions with noniterative triple excitations [CCSD-(T)][70] and by density functional methods using BLYP,[71,72] B3LYP,[72,73] PW91[74] and PBE[75] functionals. The basis set superposition error (BSSE) was corrected for all calculations with the counterpoise method.[76,77]

The MP2 level interaction energy at the basis set limit [$E_{MP2(limit)}$] was estimated by Helgaker's method and by Feller's method.[65,66] In Helgaker's method, the calculated MP2 interaction energies with Dunning's correlation consistent basis sets were fitted to the form $a + bX^{-3}$ (where X is 2 for cc-pVDZ, 3 for cc-pVTZ, etc). The $E_{MP2(limit)}$ was then estimated by extrapolation. The Helgaker's method was originally proposed for the estimation of electron correlation contribution at the basis set limit. But we have used this method for the estimation of $E_{MP2(limit)}$, as the basis set dependence of the HF level interaction energy is negligible. The $E_{MP2(limit)}$ was also estimated using the form $a + b \exp(-cX)$ proposed by Feller.

IV. Results and Discussion

A. Benzene-h_6−Methane. Figure 1 shows the MATI spectra of (a) bare benzene-h_6 and (b)−(c) the benzene-h_6−methane cluster around their first ionization potentials (IP_0). Each spectrum represents the plot of the MATI ion intensity versus the excess vibrational energy from the zero vibrational level of each cationic state (i.e., [total laser excitation energy − IP_0]).

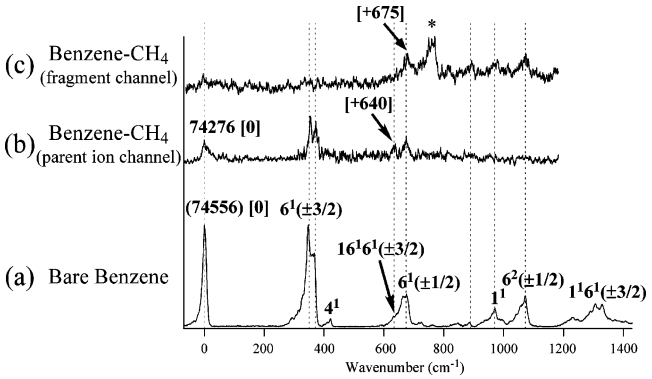

Figure 1. MATI spectra of (a) bare benzene excited via S_1 6^1, (b)−(c) benzene−methane excited via S_1 6^1. Spectra (b) and (c) were measured by monitoring the parent ion channel and fragment ion channel, respectively. Numbers in brackets are excess energies from the origin (IP_0). The asterisked band is due to the monomer fragment produced in the S_1 state (see text).

TABLE 1: Observed Band Frequencies in the MATI Spectra of Bare Benzene and the Benzene−Methane Cluster with Their Assignments[a]

assignment	bare benzene (cm^{-1})	benzene−methane cluster (cm^{-1})
0 (IP_0)	0 (74556)	0 (74276)
$6^1(\pm3/2)$	350	355
	365	370
4^1	420	
$16^16^1(\pm3/2)$	635 (shoulder)	640
$6^1(\pm1/2)$	670	675
*		(760)
16^3 or 10	840	
16^3 or 12	885	890
5^1	935	
1^1	970	975
$6^2(\pm1/2)$	1070	1075
$6^3(\pm3/2)$	1230	
$1^16^1(\pm3/2)$	1300	
	1320	

[a] The band positions are represented by the relative frequencies to each origin band (IP_0). The asterisked band is attributed to the origin band of the S_1 0^0 fragment monomer (see text).

All the spectra were measured by the two-color two-photon excitation via the S_1 6^1 intermediate state of these species. The S_1-S_0 6^1_0 band of the cluster was first reported by Schauer and Bernstein,[60] and this cluster band is low-frequency shifted by 41 cm^{-1} from the corresponding band of bare benzene. Although (b) was measured by monitoring the parent MATI ion (cluster ion), the fragment MATI ion (monomer ion) was detected in (c).

MATI spectra of bare benzene via the S_1 6^1 level have been reported by Krause et al. and Burrill et al.[78,79] In addition, high-resolution zero kinetic energy (ZEKE) photoelectron spectra have also been reported by Linder et al.[80,81] The present MATI spectrum of bare benzene is essentially the same as those previously reported, though the resolution of the present spectrum is rather moderate. According to the previously reported MATI spectra, the $16^16^1(\pm3/2)$ band (+635 cm^{-1}) appears in the low-frequency side of the $6^1(\pm1/2)$ band (+670 cm^{-1}).[78,79] These two bands, however, cannot be fully separated in the present spectrum. Table 1 summarizes the observed band positions in the MATI spectrum of bare benzene and their assignments.

It has been known that IP_0 measured by MATI spectroscopy shows a small low-frequency shift depending on the applied electric field. This is because of the energy difference between the field ionizing high Rydberg states, which contribute to the MATI signal, and the actual ionization potential, so that the extrapolation to the field free value has to be performed for the accurate determination of the ionization potential.[62] The field free IP_0 value of bare benzene has been precisely determined to be 74 556 cm^{-1}.[82] In the present MATI measurement, IP_0 of the benzene−methane cluster was calibrated to include the field ionization correction. The field free IP_0 value of bare benzene was used as the energy standard for the correction. Then, field free IP_0 of benzene−methane was determined to be 74 276 cm^{-1} on the basis of the MATI spectrum. In comparison with that of the bare molecule, the IP_0 of the cluster is low-frequency shifted by 270 cm^{-1}. This means the intermolecular interaction energy in the cation is larger than that in the neutral ground state. The enhancement of the intermolecular interaction upon ionization is well explained by the strong induction effect in the cation. The MATI spectra of the cluster show vibrational structure very similar to that of the monomer cation, except for the appearance of the asterisked band (the origin of the asterisked band will be discussed later). No remarkable changes of the intramolecular vibrational frequencies in the cluster indicate a small perturbation to the structure of the benzene moiety by the cluster formation. Moreover, no clear intermolecular vibrational modes are seen in the cluster spectra. Though this is somewhat surprising if we consider the large enhancement of the interaction energy in the cation, similar behavior has been reported also in the benzene−rare gas clusters.[83]

A striking feature of the MATI spectra of the benzene−methane cluster is the switching of the ion appearance channel with increase of the vibrational energy. The bands higher than the $6^1(\pm1/2)$ band (+675 cm^{-1}) are absent in the parent cluster ion channel (spectrum b), whereas only the bands higher than the $16^16^1(\pm3/2)$ band (+640 cm^{-1}) appear in the fragment ion channel (spectrum c). Such a change of the ion appearance channel clearly shows the predissociation of the ion core.

Because the $6^1(\pm1/2)$ band (+675 cm^{-1}) is the lowest frequency band appearing in the fragment channel, an upper limit of the dissociation threshold of the cluster cation was found to be 675 cm^{-1}. The $6^1(\pm1/2)$ band is seen also in the parent ion channel. Though it is very unusual in MATI spectra that the same band appears in two ion channels,[63] it would be interpreted as follows: the $6^1(\pm1/2)$ level lies just above the dissociation threshold and the predissociation rate is extremely slow. A fraction of the clusters excited to this level survives until the application of the pulsed acceleration field (7 μs after the excitation) and appears in the parent ion channel. On the other hand, the lowest missing band in the fragment channel is the $16^16^1(\pm3/2)$ band, which appears at + 640 cm^{-1} only in the parent ion channel. This band gives us a lower limit of the dissociation threshold. Thus, we conclude that the binding energy of the benzene−methane cluster in the cationic ground state (D_0 (cation)) must be lying in the range 640−675 cm^{-1}.

The energy scheme of bare benzene and the benzene−methane cluster is shown in Figure 2a. The binding energy of the cluster in the neutral ground state ($D_0(S_0)$) is readily evaluated by the following energy relation,

$$D_0(S_0) + IP_0(\text{monomer}) = D_0(\text{cation}) + IP_0(\text{cluster})$$

Because IP_0's of bare benzene and the cluster are 74 556 and 74 276 cm^{-1}, respectively, and the range of D_0(cation) is obtained above, $D_0(S_0)$ of the cluster is determined to be in the range 360−395 cm^{-1} (1.03−1.13 kcal/mol). This value can be regarded as the CH/π interaction energy between benzene and

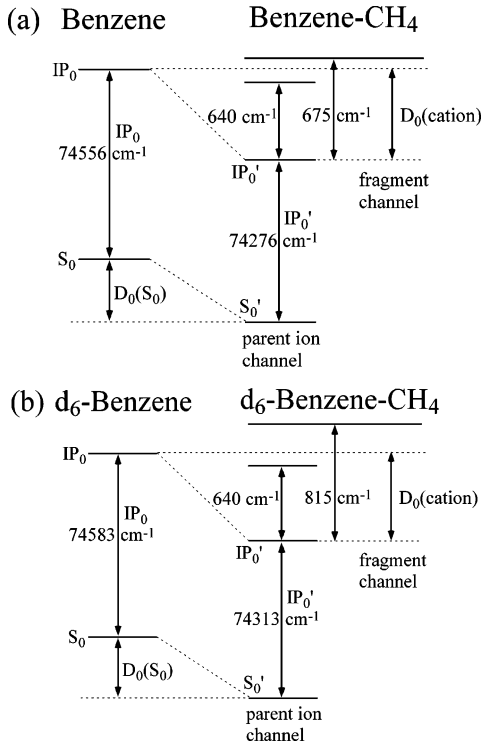

Figure 2. Energy schemes for (a) benzene−methane and (b) benzene-d_6−methane clusters.

methane. To our knowledge, this is the first experimental determination of the accurate CH/π interaction energy in the gas phase.

The experimentally determined CH/π interaction energy (1.03−1.13 kcal/mol) in the benzene−methane system is in the typical energy range for van der Waals interactions. For example, the upper limit for the interaction energy between benzene and Kr has been determined to be <1.15 kcal/mol by MATI spectroscopy.[78] The polarizability of Kr (2.48×10^{-24} cm^3) is close to that of methane (2.59×10^{-24} cm^3),[84] and the similar magnitude of the interaction energies suggests that the contribution of the dispersion interaction is dominant in the CH/π interaction.

In the end of this section, we comment on the origin of the asterisked band in the MATI spectrum of the cluster in the fragment channel. The asterisked band, which locates at +760 cm^{-1} relative to the origin of the cluster cation, is the most intense band in this spectrum. No corresponding band, however, is seen in the MATI spectrum of bare benzene, and no progression associated with this band is also seen. Therefore, this band is hardly attributed to an inter- or intramolecular vibrational mode in the cluster cation. In the measurement of this MATI spectrum, the cluster was excited via the S_1 6^1 level. The low-frequency shift of the S_1-S_0 electronic transition upon the cluster formation with methane is 41 cm^{-1}.[60] Therefore, the binding energy of the cluster in the S_1 state is estimated in the rage of 401 < $D_0(S_1)$ < 436 cm^{-1}. Because the vibrational energy of the mode 6 in S_1 is 521 cm^{-1},[85] a fraction of the cluster species in the S_1 6^1 level would predissociate prior to the excitation to high Rydberg states. When the predissociation occurs, the unique dissociation channel is the production of the benzene monomer in the S_1 vibrational ground level (0^0). Then, the cation−S_1 origin band of the monomer would appear in the MATI spectrum of the cluster by monitoring the fragment (monomer fragment) channel. To confirm this possibility, we observed the MATI spectrum of bare benzene via the S_1 0^0 level.

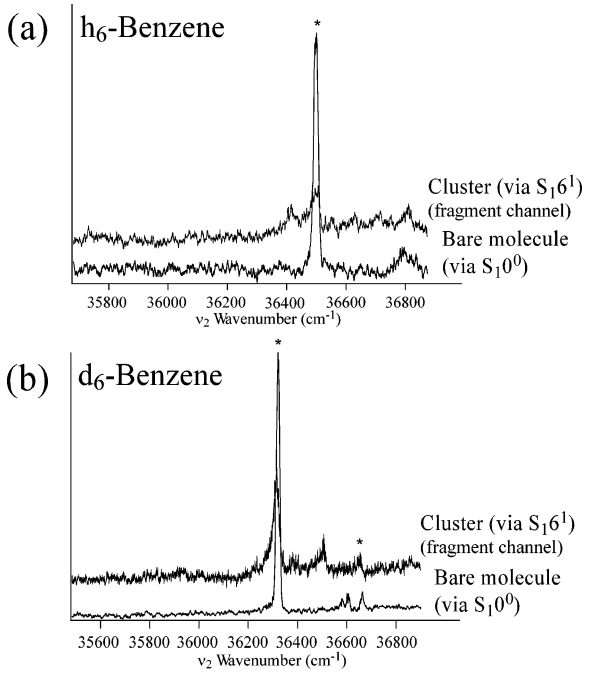

Figure 3. Comparison between the MATI spectra of bare benzene via the S_1 0^0 level and benzene−methane (fragment channel) via the $S_1 6^1$ level: (a) benzene-h_6 and (b) benzene-d_6. All the spectra are plotted with respect to the second excitation laser wavenumber.

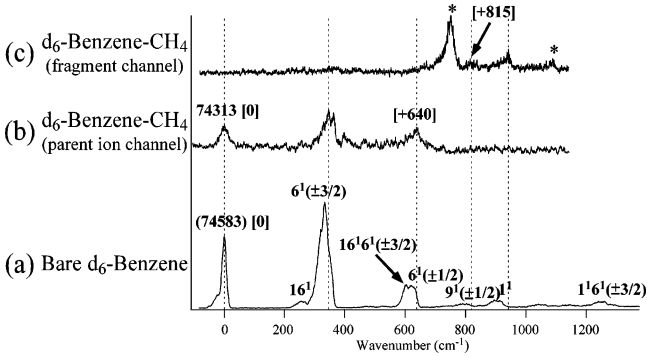

Figure 4. MATI spectra of (a) bare benzene-d_6 excited via S_1 6^1 and (b)−(c) benzene-d_6−methane excited via S_1 6^1. (b) and (c) were measured by monitoring the parent ion channel and fragment ion channel, respectively. Numbers in brackets are excess energies from the origin (IP_0). The asterisked bands are due to the monomer fragment produced in the S_1 state (see text).

Because the S_1-S_0 origin band is forbidden in benzene, we used the S_1-S_0 6^0_1 hot band to pump bare benzene to the S_1 0^0 level.[86] Figure 3a shows the comparison between the MATI spectrum of bare benzene via S_1 0^0 and that of the cluster via S_1 6^1 in the fragment channel. In this comparison, the abscissa of the spectra is plotted with respect to the second excitation laser wavenumber (ν_2). The band position of the asterisked band in the cluster spectrum agrees with the cation−S_1 origin band of the bare benzene spectrum. This clearly demonstrates that the asterisked band in the cluster MATI spectrum arises from the transition of the monomer fragment produced by the predissociation in the S_1 state.

B. Benzene-d_6−Methane. For further confirmation of the results on benzene-h_6−methane, we also measured MATI spectra of an isotopomer of the cluster, benzene-d_6−methane. Figure 4 shows the MATI spectra of (a) bare benzene-d_6 and (b)−(c) benzene-d_6−methane cluster. Spectrum a was measured by the excitation via the S_1 6^1 level of bare benzene-d_6. Both spectra b and c were obtained by the excitation via the S_1 6^1

TABLE 2: Observed Band Frequencies in the MATI Spectra of Bare Benzene-d_6 and the Benzene-d_6−Methane Cluster with Their Assignments[a]

assignment	bare benzene-d_6 (cm^{-1})	benzene-d_6−methane cluster (cm^{-1})
0 (IP_0)	0 (74583)	0 (74313)
16^1	250	
$6^1(\pm 3/2)$	335	345
		365
$16^16^1(\pm 3/2)$	600	
$6^1(\pm 1/2)$	620	640
*		(750)
$9^1(\pm 1/2)$	795	815
$16^16^1(\pm 3/2)$	900	
1^1	920	940
*		(1090)
$1^16^1(\pm 3/2)$	1260	

[a] The band positions are represented by the relative frequencies to each origin band (IP_0). The asterisked bands are attributed to the origin and $6^1(\pm 3/2)$ bands of the S_1 0^0 fragment monomer (see text).

level of benzene-d_6−methane, and the parent cluster ion and fragment monomer ions were detected, respectively. The observed band positions in the MATI spectra of the deuterated isotopomers are summarized in Table 2 with their assignments. The field ionization correction of the IP_0 value of the cluster was carried out by using field free IP_0 of benzene-d_6 (74 583 cm^{-1}) in the reference.[82] IP_0 of benzene-d_6−methane was determined to be 74 313 cm^{-1} by the MATI spectrum.

The gross feature in the MATI spectrum of the bare benzene-d_6 isotopomer is quite similar to that of benzene-h_6, but small frequency shifts are seen upon the deuteration. The $6^1(\pm 1/2)$ band is low-frequency shifted by 50 cm^{-1}. In the cluster spectrum of the fragment channel (spectrum c in Figure 4), the asterisked bands at +750 and +1090 cm^{-1} are not attributed to the transitions in the cluster. As was discussed in the previous section, these bands arise from the monomer fragment produced by the predissociation in the S_1 state. This is proved by the MATI spectrum of bare benzene-d_6 via the S_1 0^0 level shown in Figure 3b, in comparison with the spectrum of the cluster via the S_1 6^1 level. When the asterisked bands in the cluster spectrum are ignored, the spectral feature of the cluster well corresponds to that of the bare molecule. The spectral overlap of the $6^1(\pm 1/2)$ band in the parent and fragment ion channels is lift by the deuteration, and the dissociation threshold is more obvious in the isotopomer. Although the bands higher than the $6^1(\pm 1/2)$ band (+640 cm^{-1}) are absent in the parent ion channel, the bands lower than the $9^1(\pm 1/2)$ band (+815 cm^{-1}) are missing in the fragment ion channel. Therefore, we conclude that the dissociation threshold of benzene-d_6−methane in the cationic state (D_0(cation)) must lie in the range of 640−815 cm^{-1}. The energy scheme of bare benzene-d_6 and benzene-d_6−methane is shown in Figure 2b. From this scheme, the binding energy of benzene-d_6−methane in the neutral ground state (D_0-(S_0)) is determined to be in the range 370−545 cm^{-1} (1.06−1.56 kcal/mol). This binding energy is that measured from the zero point level, and the shift of the zero point energy is a unique factor for the change upon the deuteration. Though this energy region overlaps with that for benzene-h_6−methane, the large energy gap between the $6^1(\pm 1/2)$ and $9^1(\pm 1/2)$ bands prevents us from more precise determination of the energy. The binding energy of the isotopomer cluster would be quite close to that of the h_6-cluster, as will be estimated in the next section.

C. Theoretical Calculations of the Interaction Energy and Comparison with Experimental Results. Intermolecular interaction energy of the C_{3v} benzene−methane cluster

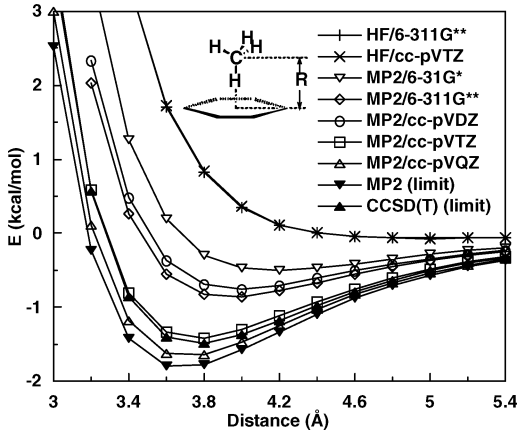

Figure 5. Comparison of calculated HF and MP2 interaction energies using 6-31G*, 6-311G* and cc-pVXZ (X = D, T and Q) basis sets with the estimated MP2 and CCSD(T) level interaction energies at the basis set limit [$E_{MP2(limit)}$ and $E_{CCSD(T)(limit)}$]. See text.

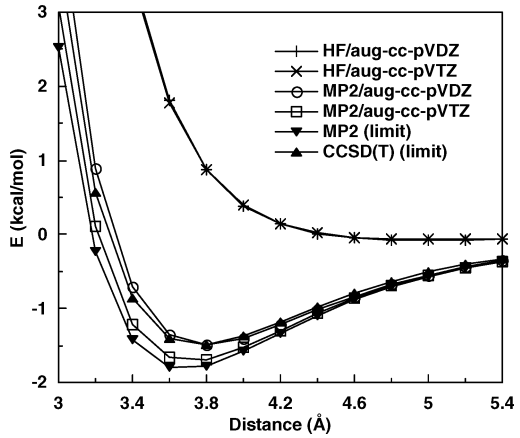

Figure 6. Comparison of calculated HF and MP2 interaction energies using aug-cc-pVXZ (X = D and T) basis sets with the estimated MP2 and CCSD(T) level interaction energies at the basis set limit [$E_{MP2(limit)}$ and $E_{CCSD(T)(limit)}$]. See text.

(Figure 5) was calculated using several basis sets at the HF and MP2 levels for evaluating the effects of basis set and electron correlation correction. The geometries of the benzene and methane monomers were optimized at the MP2/6-31G* level. The optimized monomer geometries were used for the calculations of the cluster.

The basis set dependence of HF interaction energy is negligible, whereas MP2 interaction energy depends strongly on the basis set. Small basis sets (6-31G*, 6-311G** and cc-pVDZ) underestimate the attraction greatly. The significant basis set dependence shows that a large basis set near saturation is necessary for accurate evaluation of the CH/π interaction.

The estimated MP2 interaction energies at the basis set limit [$E_{MP2(limit)}$] are also shown in Figures 5 and 6. The $E_{MP2(limit)}$ was estimated by Helgaker's method from the calculate MP2 interaction energies using the cc-pVXZ (X = T and Q) and aug-cc-pVXZ (X = D and T) basis sets in Figures 5 and 6, respectively.[65] The calculated MP2 interaction energies using the cc-pVQZ and aug-cc-pVTZ basis sets are very close to the estimated $E_{MP2(limit)}$ (Figures 5 and 6), and it shows that these basis sets are close to saturation.

Recent CCSD(T) calculations of the interaction energies of aromatic molecules show that the MP2 method overestimates the attraction compared with the more reliable CCSD(T) method.[47,49,87] We have estimated the CCSD(T) interaction energy at the basis set limit [$E_{CCSD(T)(limit)}$] by the equation

$$E_{CCSD(T)(limit)} = E_{MP2(limit)} + \Delta CCSD(T)$$

where $\Delta CCSD(T)$ ($=E_{CCSD(T)} - E_{MP2}$) is the CCSD(T) correction term (the difference between the CCSD(T) and MP2 interaction energies).[47] Previous calculations of the benzene−methane cluster show that the basis dependence of $\Delta CCSD(T)$ is not large.[47] The $\Delta CCSD(T)$ was calculated using the cc-pVDZ basis set. The estimated $E_{CCSD(T)(limit)}$ values are also shown in Figures 5 and 6. The MP2/cc-pVTZ and MP2/aug-cc-pVDZ level interaction energies are very close to the $E_{CCSD(T)(limit)}$. Although the cc-pVTZ and aug-cc-pVDZ basis sets underestimate the attraction compared with a larger basis set near saturation, the MP2 calculations overestimate the attraction compared with the CCSD(T) calculations. Apparently error cancellation is the cause of the good performance of the MP2 calculations using these basis sets. The HF calculations underestimate the attraction considerably compared with the estimated $E_{CCSD(T)(limit)}$. The large gain of the attraction by electron correlation correction indicates that the dispersion interaction is mainly responsible for the attraction.

The binding energy (D_0) of the benzene−methane cluster was calculated from an $E_{CCSD(T)(limit)}$ (D_e) and vibrational zero-point energies (ZPE's). The geometry of the cluster was optimized at the MP2/cc-pVTZ level. The MP2 interaction energy of the optimized cluster was calculated using Dunning's correlation consistent basis sets as summarized in Table 3. The $E_{MP2(limit)}$ estimated by Helgaker's method from the MP2/aug-cc-pVXZ (X = T and Q) level interaction energies was −1.803 kcal/mol. A nearly identical $E_{MP2(limit)}$ was obtained from the MP2/cc-pVXZ (X = T and Q) calculations (−1.820 kcal/mol) and from the MP2/aug-cc-pVXZ (X = D and T) calculations (−1.790 kcal/mol). The $E_{MP2(limit)}$ from MP2/cc-pVXZ (X = D and T) calculations (−1.734 kcal/mol) and that estimated by Feller's method from the MP2/cc-pVXZ (X = D, T and Q) calculations (−1.753 kcal/mol) are slightly (0.05−0.07 kcal/mol) smaller.

The $E_{CCSD(T)(limit)}$ was calculated from the $E_{MP2(limit)}$ (−1.803 kcal/mol) and the $\Delta CCSD(T)$ obtained using the cc-pVTZ basis set (0.375 kcal/mol). The estimated $E_{CCSD(T)(limit)}$ (D_e) was −1.428 kcal/mol. The $E_{CCSD(T)(limit)}$ estimated by Helgaker's method from the CCSD(T)/cc-pVXZ (X = D and T) calculations (−1.330 kcal/mol) is slightly (0.10 kcal/mol) smaller. The estimation by Helgaker's method from the calculations using the cc-pVXZ (X = D and T) basis sets would be the cause of the slightly smaller $E_{CCSD(T)(limit)}$ as in the case of the estimation of $E_{MP2(limit)}$.[88]

The ZPE's of benzene, methane monomers and benzene−methane cluster calculated at the MP2/cc-pVTZ level are 63.199, 28.496 and 91.991 kcal/mol, respectively. The change of ZPE's by the formation of the dimer (ΔZPE) is 0.296 kcal/mol.[89] The estimated D_0 ($=D_e - \Delta$ZPE, 1.132 kcal/mol) agrees well with the experimental D_0 (1.03−1.13 kcal/mol). The good agreement shows that high-level ab initio calculations using a very large basis set and CCSD(T) level electron correlation provide very accurate CH/π interaction energy. The ZPE's of benzene-d_6 and benzene-d_6−methane are 50.847 and 79.634 kcal/mol, respectively. The ΔZPE is 0.291 kcal/mol. The estimated D_0 of the benzene-d_6−methane cluster is 1.137 kcal/mol, and this is also consistent with the experimental evaluation.

The calculated potentials in Figures 5 and 6 indicate that MP2/cc-pVXZ (X = T or Q) or MP2/aug-cc-pVXZ (X = D or T) level calculation is necessary for quantitative evaluation of the CH/π interaction energy. Smaller basis sets (6-31G*, 6-311G** and cc-pVDZ) are not appropriate for quantitative evaluation, as these basis sets underestimate the attraction considerably. These basis sets may possibly be used for qualitative analysis of the CH/π interaction energy. HF calculation is not suitable for the evaluation of the CH/π interaction energy, as the dispersion interaction is the major source of the attraction.

TABLE 3: Calculated MP2 and CCSD(T) Interaction Energies of the Benzene−Methane Cluster and the Estimated MP2 and CCSD(T) Interaction Energies at the Basis Set Limit (See Text)[a]

method		energy
E_{MP2}[b]		
cc-pVDZ	1	−0.654
cc-pVTZ	2	−1.414
cc-pVQZ	3	−1.649
aug-cc-pVDZ	4	−1.483
aug-cc-pVTZ	5	−1.699
aug-cc-pVQZ	6	−1.759
$E_{CCSD(T)}$[c]		
cc-pVDZ	7	−0.348
cc-pVTZ	8	−1.039
aug-cc-pVDZ	9	−1.155
$E_{MP2(limit)}$[d]		
Helgaker using **1** and **2**[e]	10	−1.734
Helgaker using **2** and **3**[e]	11	−1.820
Helgaker using **4** and **5**[e]	12	−1.790
Helgaker using **5** and **6**[e]	13	−1.803
Feller using **1, 2** and **3**[f]	14	−1.753
Feller using **4, 5** and **6**[f]	15	−1.782
$\Delta CCSD(T)$[g]		
cc-pVDZ (**7** − **1**)	16	0.307
cc-pVTZ (**8** − **2**)	17	0.375
aug-cc-pVDZ (**9** − **4**)	18	0.329
$E_{CCSD(T)(limit)}$[h]		
13 + **17**	19	−1.428
Helgaker using **7** and **8**[e]	20	−1.330

[a] Energy in kcal/mol. BSSE was corrected by the counterpoise method. The MP2/cc-pVTZ level optimized geometry was used. See text. [b] Calculated MP2 level interaction energy. [c] Calculated CCSD(T) level interaction energy. [d] Estimated MP2 level interaction energy at the basis set limit. [e] Helgaker's method is used for the estimation. See text. [f] Feller's method is used for the estimation. See text. [g] CCSD(T) correction term $\Delta CCSD(T) = E_{CCSD(T)} - E_{MP2}$. See text. [h] Estimated CCSD(T) level interaction energy at the basis set limit.

DFT calculations were often used for the evaluation of the CH/π interaction energy.[3,4,56−58,90,91] But DFT calculations with commonly used functionals cannot accurately evaluate the dispersion interaction.[92−94] Detailed evaluation of the accuracy of the calculated CH/π interaction energy by DFT methods has not yet been reported.[95] The interaction energy of the cluster was calculated by DFT methods using BLYP, B3LYP, PW91 and PBE functionals. The calculated interaction energies are compared with the $E_{MP2(limit)}$ and $E_{CCSD(T)(limit)}$ as shown in Figure 7. The BLYP and B3LYP potentials are close to the HF potential. The BLYP and B3LYP calculations cannot evaluate the attraction, as in the cases of rare gas and methane dimers.[93] The PW91 and PBE potentials have shallow minima. But the calculated attraction with these functionals are considerably smaller than that obtained by the CCSD(T) calculations. The comparison clearly shows that DFT calculations with these functionals are not appropriate for the quantitive evaluation of the CH/π interaction energy.

V. Conclusion

In this paper, we reported the MATI spectra of bare benzene, benzene-d_6, benzene−methane, and benzene-d_6−methane. The dissociation thresholds of benzene−methane and benzene-d_6−methane in the cationic state were determined by the MATI spectra, and the binding energies of the clusters in the neutral ground state were evaluated. These values are regarded as the

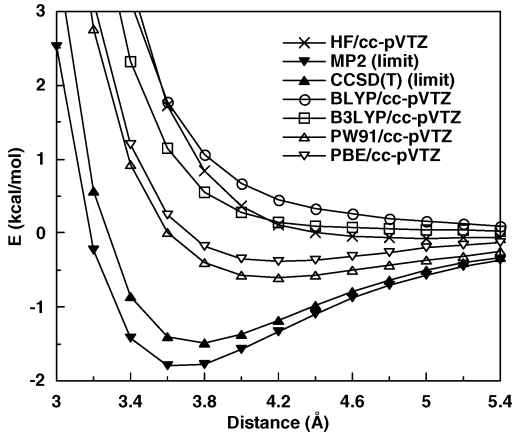

Figure 7. Comparison of calculated interaction energies by DFT methods using BLYP, B3LYP, PW91 and PBE functionals with the estimated MP2 and CCSD(T) level interaction energies at the basis set limit [$E_{MP2(limit)}$ and $E_{CCSD(T)(limit)}$]. See text.

CH/π interaction energy in the benzene−methane model system, and this is the first experimental determination of the accurate CH/π interaction energy in the gas phase. The calculated binding energy by the high-level ab initio method agreed well with the experimental binding energy. A large basis set and electron correlation correction is necessary for quantitative evaluation of the CH/π interaction energy. DFT calculations using BLYP, B3LYP, PW91 and PBE functionals are not appropriate for the evaluation of the CH/π interaction energy, as these methods cannot accurately evaluate the dispersion interaction.

Acknowledgment. This work was partially supported by the MEXT Japan through projects (Nos. 1600200 and 17310057) of the Grant-in-Aid. We thank Tsukuba Advanced Computing Center for the provision of the computational facilities. This work was also partly supported by NAREGI Nanoscience Project, Ministry of Education, Culture, Sports, Science and Technology.

References and Notes

(1) Nishio, M.; Hirota, M.; Umezawa, Y. *The CH/π Interaction*; Wiley-VCH: New York, 1998.
(2) Desiraju, G. R.; Steiner, T. *The Weak Hydrogen Bond*; Oxford University Press: New York, 1999.
(3) Yamakawa, M.; Yamada, I.; Noyori, R. Angew. *Chem. Int. Ed*. **2001**, *40*, 2818.
(4) Ujaque, G.; Lee, P. S.; Houk, K. N.; Hentemann, M. F.; Danishefsky, S. J. *Chem. Eur. J*. **2002**, *8*, 3423.
(5) Nishio, M. *Tetrahedron* **2005**, *61*, 6923.
(6) Kodama, Y.; Nishihata, K.; Nishio, M.; Nakagawa, N. *Tetrahedron Lett*. **1977**, 2105.
(7) Kodama, Y.; Nishihata, K.; Nishio, M.; Iitaka, Y. *J. Chem. Soc., Perkin Trans. 2* **1976**, 1490.
(8) Hirota, M.; Takahashi, Y.; Nishio, M.; Nishihata, K. *Bull. Chem. Soc. Jpn*. **1978**, *51*, 2358.
(9) Kodama, Y.; Nishihata, K.; Nishio, M.; Uzawa, J.; Sakamoto, K.; Iwamura, H. *Bull. Chem. Soc. Jpn*. **1979**, *52*, 2661.
(10) Kodama, Y.; Zushi, S.; Nishihata, K.; Nishio, M.; Uzawa, J. *J. Chem. Soc., Perkin Trans. 2* **1980**, 1306.
(11) Uzawa, J.; Zushi, S.; Kodama, Y.; Fukuda, Y.; Nishihata, K.; Umemura, K.; Nishio, M.; Hirota, M. *Bull. Chem. Soc. Jpn*. **1980**, *53*, 3623.
(12) Zushi, S.; Kodama, Y.; Nishihata., K.; Umemura, K.; Nishio, M.; Uzawa, J.; Hirota, M. *Bull. Chem. Soc. Jpn*. **1980**, *53*, 3631.
(13) Hirota, M.; Sekiya, T.; Abe, K.; Tashiro, H.; Karatsu, M.; Nishio, M.; Osawa, E. *Tetrahedron* **1983**, *39*, 3091.
(14) Takahashi, O.; Yasunaga, K.; Gondoh, Y.; Kohno, Y.; Saito, K.; Nishio, M. *Bull. Chem. Soc. Jpn*. **2002**, *75*, 1777.
(15) Takahashi, O.; Saito, K.; Kohno, Y.; Suezawa, H.; Ishihara, S.; Nishio, M. *Bull. Chem. Soc. Jpn*. **2003**, *76*, 2167.
(16) Takahashi, O.; Kohno, Y.; Saito, K.; Nishio, M. *Chem. Eur. J*. **2003**, *9*, 756.
(17) Quiocho, F. A.; Vyas, N. K. *Nature* **1984**, *310*, 381.
(18) Quiocho, F. A. *Annu. Rev. Biochem*. **1986**, *55*, 287.
(19) Spurlino, J. C.; Liu, G.-Y.; Quiocho, F. A. *J. Biol. Chem*. **1991**, *266*, 5202.
(20) Umezawa, Y.; Nishio, M. *Bioorg. Med. Chem*. **1998**, *6*, 493.
(21) Umezawa, Y.; Nishio, M. *Bioorg. Med. Chem*. **1998**, *6*, 2507.
(22) Umezawa, Y.; Tsuboyama, S.; Honda, K.; Uzawa, J.; Nishio, M. *Bull. Chem. Soc. Jpn*. **1998**, *71*, 1207.
(23) Umezawa, Y.; Tsuboyama, S.; Takahashi, H.; Uzawa, J.; Nishio, M. *Tetrahedron* **1999**, *55*, 10047.
(24) Ungaro, R.; Pochini, A.; Andreetti, G. D.; Sangermano, V. *J. Chem. Soc., Perkin Trans. 2* **1984**, 1979.
(25) Kobayashi, K.; Asakawa, Y.; Kato, Y.; Aoyama, Y. *J. Am. Chem. Soc*. **1992**, *114*, 10307.
(26) Kobayashi, K.; Asakawa, Y.; Kikuchi, Y.; Toi, H.; Aoyama, Y. *J. Am. Chem. Soc*. **1993**, *115*, 2648.
(27) Amabilino, D. B.; Ashton, P. R.; Brown, C. L.; Cordova, E.; Godinez, L. A.; Goodnow, T. T.; Kaifer, A. E.; Newton, S. P.; Pietraszkiewicz, M.; Philip, D.; Raymo, F. M.; Reder, A. S.; Rutland, M. T.; Slawin, A. M. Z.; Spencer, N.; Stoddart, J. F.; Williams, D. J. *J. Am. Chem. Soc*. **1995**, *117*, 1271.
(28) Ballardini, R.; Balzani, V.; Credi, A.; Brown, C. L.; Gillard, R. E.; Montalti, M.; Philp, D.; Stoddart, J. F.; Venturi, M.; White, A. J. P.; Williams, B. J.; Williams, D. J. *J. Am. Chem. Soc*. **1997**, *119*, 12503.
(29) Asakawa, M.; Ashton, P. R.; Hayes, W.; Janssen, H. M.; Meijer, E. W.; Menzer, S.; Pasini, D.; Stoddart, J. F.; White, A. J. P.; Williams, D. J. *J. Am. Chem. Soc*. **1998**, *120*, 920.
(30) Meyer, E. A.; Castellano, R. K.; Diederich, F. *Angew. Chem., Int. Ed*. **2003**, *42*, 1210.
(31) Frontera, A.; Garau, C.; Quinonero, D.; Ballester, P.; Costa, A.; Deya, P. M. *Org. Lett*. **2003**, *5*, 1135.
(32) Re, S.; Nagase, S.*J. Chem. Soc., Chem. Commun*. **2004**, 658.
(33) Suezawa, H.; Yoshida, T.; Hirota, M.; Takahashi, H.; Umezawa, Y.; Honda, K.; Tsuboyama, S.; Nishio, M. *J. Chem. Soc., Perkin Trans. 2* **2001**, 2053.
(34) Matsumoto, A.; Tanaka, T.; Tsubouchi, T.; Tashiro, K.; Saragai, S.; Nakamoto, S. *J. Am. Chem. Soc*. **2002**, *124*, 8891.
(35) Kobayashi, Y.; Kurasawa, T.; Kinbara, K.; Saigo, K. *J. Org. Chem*. **2004**, *69*, 7436.
(36) Nishio, M. *Cryst. Eng. Commun*. **2004**, *6*, 130.
(37) Yoshida, Y.; Muroi, K.; Otsuka, A.; Saito, G.; Takahashi, M.; Yoko, T. *Inorg. Chem*. **2004**, *43*, 1458.
(38) Kobayashi, Y.; Saigo, K. *J. Am. Chem. Soc*. **2005**, *127*, 15054.
(39) Yamamoto, Y.; Yamamoto, A.; Furuta, S.; Horie, M.; Kodama, M.; Sato, W.; Akiba, K. Y.; Tsuzuki, S.; Uchimaru, T.; Hashizume, D.; Iwasaki, F. *J. Am. Chem. Soc*. **2005**, *127*, 14540.
(40) Brandl, M.; Weiss, M. S.; Jabs, A.; Suhnel, J.; Hilgenfeld, R. *J. Mol. Biol*. **2001**, *307*, 357.
(41) Toth, G.; Murphy, R. F.; Lovas, S. *Protein Eng*. **2001**, *14*, 543.
(42) Umezawa, Y.; Nishio, M. *Nucl. Acids Res*. **2002**, *30*, 2183.
(43) Mori, A.; Hirayama, K.; Kato, N.; Takeshita, A.; Ujiie, S. *Chem. Lett*. **1997**, 509.
(44) Takagi, T.; Tanaka, A.; Matsuo, S.; Maezaki, H.; Tani, M.; Fujiwara, H.; Sasaki, Y. *J. Chem. Soc., Perkin Trans. 2* **1987**, 1015.
(45) Sakai, S.; Kato, K.; Miyazaki, T.; Musashi, Y.; Ohkubo, K.; Ihara, H.; Hirayama, C. *J. Chem. Soc., Faraday Trans*. **1993**, *89*, 659.
(46) Tsuzuki, S.; Honda, K.; Uchimaru, T.; Mikami, M.; Tanabe, K. *J. Phys. Chem. A* **1999**, *103*, 8265.
(47) Tsuzuki, S.; Honda, K.; Uchimaru, T.; Mikami, M.; Tanabe, K. *J. Am. Chem. Soc*. **2000**, *122*, 3746.
(48) Tarakeshwar, P.; Choi, H. S.; Kim, K. S. *J. Am. Chem. Soc*. **2001**, *123*, 3323.
(49) Tsuzuki, S.; Honda, K.; Uchimaru, T.; Mikami, M.; Tanabe, K. *J. Phys. Chem. A* **2002**, *106*, 4423.
(50) Takahashi, O.; Kohno, Y.; Iwasaki, S.; Saito, K.; Iwaoka, M.; Tomoda, S.; Umezawa, Y.; Tsuboyama, S.; Nishio, M. *Bull. Chem. Soc. Jpn*. **2001**, *74*, 2421.
(51) Takahashi, O.; Kohno, Y.; Saito, K. *Chem. Phys. Lett*. **2003**, *378*, 509.
(52) Oki, M.; Takano, S.; Toyota, S. *Bull. Chem. Soc. Jpn*. **2000**, *73*, 2221.
(53) Kim, K. S.; Tarakeshwar, P.; Lee, J. Y. *Chem. Rev*. **2000**, *100*, 4145.
(54) Tsuzuki, S.; Houjou, H.; Nagawa, Y.; Hiratani, K. *J. Chem. Soc., Perkin Trans. 2* **2001**, 1951.
(55) Ribas, J.; Cubero, E.; Luque, F. J.; Orozco, M. J. *J. Org. Chem*. **2002**, *67*, 7057.
(56) Ugozzoli, F.; Arduini, A.; Massera, C.; Pochini, A.; Secchi, A. *New J. Chem*. **2002**, *26*, 1718.
(57) Sundararajan, K.; Sankaran, K.; Viswanathan, K. S.; Kulkarni, A. D.; Gadre, S. R. *J. Phys. Chem. A* **2002**, *106*, 1504.
(58) Sundararajan, K.; Viswanathan, K. S.; Kulkarni, A. D.; Gadre, S. R. *J. Mol. Struct*. **2002**, *613*, 209.

(59) Ehama, R.; Tsushima, M.; Yuzuri, T.; Suezawa, H.; Sakakibara, K.; Hirota, M. *Bull. Chem. Soc. Jpn*. **1993**, *66*, 814.
(60) Schauer, M.; Bernstein, E. R. *J. Chem. Phys*. **1985**, *82*, 726.
(61) Zhu, L.; Johnson, P. M. *J. Chem. Phys.* **1991**, *94*, 5769.
(62) Schlag, E. W. *ZEKE Spectroscopy*; Cambridge University Press: Cambridge, U.K., 1998.
(63) Grebner, Th. L.; Neusser, H. J. *Int. J. Mass Spectrom. Ion Processes* **1996**, *159*, 137.
(64) Dessent, C. E. H.; Müller-Dethlefs, K. *Chem. Rev.* **2000**, *100*, 3999.
(65) Helgaker, T.; Klopper, W.; Koch, H.; Noga, J. *J. Chem. Phys.* **1997**, *106*, 9639.
(66) Feller, D. J. *Chem. Phys*. **1992**, *96*, 6104.
(67) Frisch, M. J.; Trucks, G. W.; Schlegel, H. B.; Scuseria, G. E.; Robb, M. A.; Cheeseman, J. R.; Montgomery, J. A., Jr.; Vreven, T.; Kudin, K. N.; Burant, J. C.; Millam, J. M.; Iyengar, S. S.; Tomasi, J.; Barone, V.; Mennucci, B.; Cossi, M.; Scalmani, G.; Rega, N.; Petersson, G. A.; Nakatsuji, H.; Hada, M.; Ehara, M.; Toyota, K.; Fukuda, R.; Hasegawa, J.; Ishida, M.; Nakajima, T.; Honda, Y.; Kitao, O.; Nakai, H.; Klene, M.; Li, X.; Knox, J. E.; Hratchian, H. P.; Cross, J. B.; Bakken, V.; Adamo, C.; Jaramillo, J.; Gomperts, R.; Stratmann, R. E.; Yazyev, O.; Austin, A. J.; Cammi, R.; Pomelli, C.; Ochterski, J. W.; Ayala, P. Y.; Morokuma, K.; Voth, G. A.; Salvador, P.; Dannenberg, J. J.; Zakrzewski, V. G.; Dapprich, S.; Daniels, A. D.; Strain, M. C.; Farkas, O.; Malick, D. K.; Rabuck, A. D.; Raghavachari, K.; Foresman, J. B.; Ortiz, J. V.; Cui, Q.; Baboul, A. G.; Clifford, S.; Cioslowski, J.; Stefanov, B. B.; Liu, G.; Liashenko, A.; Piskorz, P.; Komaromi, I.; Martin, R. L.; Fox, D. J.; Keith, T.; Al-Laham, M. A.; Peng, C. Y.; Nanayakkara, A.; Challacombe, M.; Gill, P. M. W.; Johnson, B.; Chen, W.; Wong, M. W.; Gonzalez, C.; Pople, J. A. *Gaussian 03*, Revision C.02; Gaussian, Inc.: Wallingford, CT, 2004.
(68) Møller, C.; Plesset, M. S. *Phys. Rev.* **1934**, *46*, 618.
(69) Head-Gordon, M.; Pople, J. A.; Frisch, M. J.*Chem. Phys. Lett*. **1988**, *153*, 503.
(70) Pople, J. A.; Head-Gordon, M.; Raghavachari, K. *J. Chem. Phys*. **1987**, *87*, 5968.
(71) Becke, A. D. *Phys. Rev. A* **1988**, *38*, 3098.
(72) Lee, C.; Yang, W.; Parr, R. G. *Phys. Rev. B* **1988**, *37*, 785.
(73) Becke, A. D. *J. Chem. Phys.* **1993**, *98*, 5648.
(74) Perdew, J. P.; Wang, Y. *Phys. Rev. B* **1992**, *45*, 13244.
(75) Perdew, J. P.; Burke, K.; Ernzerhof, M. *Phys. Rev. Lett*. **1996**, *77*, 3865.
(76) Ransil, B. J. *J. Chem. Phys*. **1961**, *34*, 2109.
(77) Boys, S. F.; Bernardi, F. *Mol. Phys.* **1970**, *19*, 553.
(78) Krause, H.; Neusser, H. J. *J. Chem. Phys.* **1992**, *97*, 5923.
(79) Burrill, A. B.; Chung, Y. K.; Mann, H. A.; Johnson, P. M. *J. Chem. Phys*. **2004**, *120*, 8587.
(80) Linder, R.; Sekiya, H.; Beyl, B.; Müller-Dethlefs, K. *Angew. Chem., Int. Ed. Engl*. **1993**, *32*, 603.
(81) Linder, R.; Sekiya, H.; Müller-Dethlefs, K. *Angew. Chem., Int. Ed. Engl*. **1993**, *32*, 1364.
(82) Neuhauser, R. G.; Siglow, K.; Neusser, H. J. *J. Chem. Phys*. **1997**, *106*, 896.
(83) Krause, H.; Neusser, H. J. *Chem. Phys. Lett*. **1993**, *213*, 603.
(84) *CRC Handbook of Chemistry and Physics*, 76th ed.; Lide, D. R., Ed.; CRC Press: Boca Raton, FL, 1995.
(85) Page, R. H.; Shen, Y. R.; Lee, Y. T. *J. Chem. Phys*. **1988**, *88*, 5362.
(86) Stephenson, T. A.; Radloff, P. L.; Rice, S. A. *J. Chem. Phys*. **1984**, *81*, 1060.
(87) Hobza, P.; Selzle, H. L.; Schlag, E. W. *J. Phys. Chem*. **1996**, *100*, 18790.
(88) The model structure considered in this work (Figure 5) is not the unique possible orientation. Tsuzuki et al. estimated the binding energies (D_e) of six orientation clusters (ref 47). Our model structure corresponds to one of their model clusters. We have estimated the $E_{CCSD(T)(limit)}$ of five other orientation clusters to confirm that the model structure is the most stable. The estimated $E_{CCSD(T)(limit)}$ of the clusters shows that our model structure (Figure 5) is the most stable. The $E_{MP2(limit)}$ was estimated by Helgaker's method from the MP2/aug-cc-pVXZ (X = D and T) level interaction energies. ΔCCSD(T) was calculated using the cc-pVDZ basis set. The estimated $E_{CCSD(T)(limit)}$ of the five orientation complexes (B−F in Figure 1 of ref 47) are −1.285, −1.360, −0.949, −1.019 and −1.123 kcal/mol, respectively. They are smaller (less negative) than the $E_{CCSD(T)(limit)}$ of our model structure (−1.483 kcal/mol) obtained using the same procedure.
(89) ZPE's were also evaluated using scaled vibrational frequencies. The scaling does not largely change the calculated binding energy (D_0). The scaling factor of 0.95 was obtained from the comparison between the calculated frequency of the symmetric stretching mode of methane at the MP2/cc-pVTZ level (3076 cm^{-1}) and the experimental one (2917 cm^{-1}). The ΔZPE obtained using the scaled frequencies is 0.281 kcal/mol, which is only 0.015 kcal/mol smaller than that from the nonscaled ones. The change of ΔZPE by the scaling is only 1.3% of the calculated D_0.
(90) Medakovic, V. B.; Milcic, M. K.; Bogdanovic, G. A.; Zaric, S. D. *J. Inorg. Biochem*. **2004**, *98*, 1867.
(91) Linares, M.; Pellegatti, A.; Roussel, C. *J. Mol. Struct. (THEOCHEM)* **2004**, *680*, 169.
(92) Meijer, E. J.; Sprik, M. *J. Chem. Phys*. **1996**, *105*, 8684.
(93) Tsuzuki, S.; Lüthi, H. P. *J. Chem. Phys*. **2001**, *114*, 3949.
(94) Sato, T.; Tsuneda, T.; Hirao, K. *J. Chem. Phys.* **2005**, *123*, 104307.
(95) Recently, Truhlar et al. reported that the energy of weak interaction (OH/π) was estimated accurately by the DFT method using a functional modified by them. Electrostatic interaction contributes to the attraction in the OH/π interaction largely (ref 96). The large electrostatic interaction would be the cause of the good performance of their DFT calculations, as DFT calculations can evaluate electrostatic interaction sufficiently accurately. They also reported the calculations of the NH/π interaction using the same functional. Their calculations underestimate the energy of the NH/π interaction, where the contribution of the electrostatic interaction is smaller than that in the OH/π interaction.
(96) Tsuzuki, S.; Honda, K.; Uchimaru, T.; Mikami, M.; Tanabe, K. *J. Am. Chem. Soc.* **2000**, *122*, 11450.